



## Ballistic transport and Andreev resonances in Nb/In superconducting contacts to InAs and LTG-GaAs

T. RIZK<sup>†</sup>, A. YULIUS, W. I. YOO, P. F. BAGWELL, D. MCINTURFF, P. CHIN<sup>‡</sup>  
J. M. WOODALL<sup>§</sup>

*School of Electrical and Computer Engineering, Purdue University, West Lafayette, IN 47907, U.S.A.*

T. M. PEKAREK<sup>¶</sup>

*Department of Physics, Purdue University, West Lafayette, IN 47907, U.S.A.*

T. N. JACKSON

*Department Electrical and Computer Engineering, Pennsylvania State University, University Park, PA 16802-2701, U.S.A.*

*(Received 28 April 1999)*

---

We have formed superconducting contacts in which Cooper pairs incident from a thick In layer must move through a thin Nb layer to reach a semiconductor, either InAs or low temperature grown (LTG) GaAs. The effect of pair tunneling through the Nb layer can be seen by varying the temperature through the critical temperature of In. Several of the In/Nb–InAs devices display a peak in the differential conductance near zero-bias voltage, which is strong evidence of ballistic transport across the NS interface. The differential conductance of the In/Nb–LTG-GaAs materials system displays conductance resonances of McMillan–Rowell type. These resonant levels exist within a band of conducting states inside the energy gap, formed from excess As incorporation into the LTG-GaAs during growth. Electrons propagating in this band of states multiply reflect between the superconductor and a potential barrier in the GaAs conduction band to form the conductance resonances. A scattering state theory of the differential conductance, including Andreev reflections from the composite In/Nb contact, accounts for most qualitative features in the data.

© 1999 Academic Press

**Key words:** NS junction, superconductor–semiconductor, Andreev reflection, ballistic transport, McMillan–Rowell resonances.

---

<sup>†</sup>Present address: Samsung Corporation, Austin, TX 78754, U.S.A.

<sup>‡</sup>Present address: TRW Corporation, Redondo Beach, CA 90278, U.S.A.

<sup>§</sup>Present address: Yale University, Department of Electrical Engineering, New Haven, CT 06520, U.S.A.

<sup>¶</sup>Present address: Dept. of Physics, University of North Florida, Jacksonville, FL 32224, U.S.A.

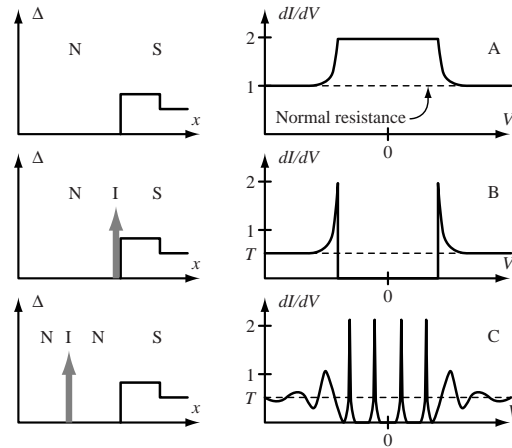


**Fig. 1.** Differential conductance for A, a ballistic NS interface; B, an NIS Giaever tunneling contact; and C, an NINS interface displaying the McMillan–Rowell resonances. Solid lines on the left indicate the pairing potential and the grey arrow an insulating (tunnel) barrier.

## 1. Introduction

Superconducting contacts to semiconductors can be used as a high resolution spectroscopy tool to understand the mechanism of ohmic contacts between metals and semiconductors. The subgap conductance of a normal-metal/superconductor (NS) interface is quite sensitive to the presence of any insulating barriers, varying with the square of the barrier transmission  $T$ , rather than proportional to  $T$  as in normal metal contacts. Also, any tunnel barriers spatially separated from the superconducting contacts give rise to pronounced conductance resonances. The Blonder–Tinkham–Klapwijk (BTK) formula [1] predicts the differential conductance of different types of NS contacts [2, 3] shown in Fig. 1.

We wish to use the insights from Fig. 1 to better understand both the superconducting properties and the ohmic contact mechanism of superconductors and metals to LTG-GaAs and InAs. This paper compares the electrical characteristics between a composite In/Nb superconducting contact formed to InAs and to LTG-GaAs. We observed clear signs of ballistic transport in many of the InAs samples, but not for the LTG-GaAs samples. However, we did observe transmission resonances in the LTG-GaAs samples indicative of a band of conducting electronic states inside the energy gap of the LTG-GaAs.

Many groups have previously studied NS junctions using GaAs as the semiconductor [4–15]. The main advantages of GaAs as the semiconductor is the ease with which one can control the geometry of the electron gas using Schottky gates and its high electron mobility. The disadvantage of GaAs is that most metals, including superconductors, form a Schottky contact. The Schottky barrier eliminates any possibility of ballistic transport through the NS interface. Low-temperature grown (LTG) GaAs has previously been investigated because of its ability to make low resistance ohmic contacts to semiconductor devices [16]. We therefore reasoned that the tunnel barrier formed at the interface between LTG-GaAs and a superconductor might be low enough to form a reasonably high transmission interface.

The energy band diagram of the superconductor/LTG-GaAs contact, along with the differential conductance one expects from the BTK formula, is shown in Fig. 2. The subgap resonances in differential conductance, shown on the right of Fig. 2, are McMillan–Rowell-type NINS resonances. Figure 2 assumes there is essentially no tunnel barrier between the In/Nb contact and the LTG-GaAs. That is, the superconductor to LTG-GaAs contact forms a nearly perfect NS interface. However, there is still a tunnel barrier which the electrons must traverse to enter the GaAs substrate, formed by the ordinary high-temperature grown GaAs. Therefore, placing a superconductor on the LTG-GaAs forms an NINS junction. If the interface between

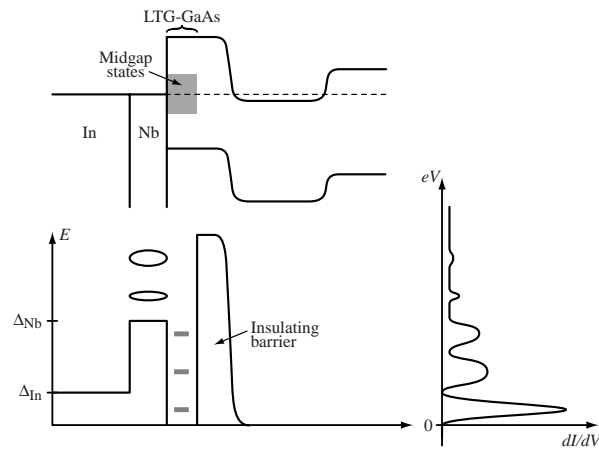


**Fig. 2.** Energy band diagram for a superconductor (In/Nb) to LTG-GaAs contact. The band of conducting states arise from excess As incorporation, which traps electrons in the GaAs between the superconductor and GaAs tunnel barrier. Expected differential conductance of the sample, including these subgap Andreev resonances, is shown on the right.

the superconductor and LTG-GaAs were not ballistic, one would simply expect Giaever tunneling in the differential conductance. Many such NIS or ‘super-Schottky’ junctions have previously been experimentally measured in superconductor/GaAs contacts.

LTG-GaAs is unique in that it contains a large number of point defects due to excess As incorporation during growth. The point defects provide an additional transmissive energy band near the middle of the semiconductor energy gap, which greatly reduces the barrier between the metal and the GaAs material [17]. In addition to the band of conducting states in the LTG-GaAs, using an LTG-GaAs layer enables us to achieve effective surface doping  $10^{20} \text{ cm}^{-3}$  rather than the limit of  $10^{18} \text{ cm}^{-3}$  in bulk GaAs. [18] This two orders of magnitude increase in the surface doping greatly reduces the Schottky barrier width between the metal and GaAs, permitting the development of low resistance ohmic contacts to GaAs not attainable using other methods.

The negative Schottky barrier formed at most metal interfaces with InAs, on the other hand, indicates that it is possible to make ballistic NS interfaces to InAs. The surface of InAs accumulates electrons, forming a natural conduction channel. The surface accumulation property of InAs is well known, and accounts for the large number of previous experiments using superconductor/InAs contacts [19–34]. The energy band diagram of the superconductor/InAs contact, along with the differential conductance one expects from the BTK formula, is shown in Fig. 3.

## 2. Experimental results

The data below shows an interplay between the thin Nb portion of the superconducting contact and the thicker In superconductor. The Nb contacts to both InAs and LTG-GaAs semiconductors in this study are 1000 Å thick, comparable to the Cooper pair size in the Nb. Andreev reflections from the superconducting contact Nb alone will therefore not be perfect, even if the NS interface is ballistic. Only when the temperature is also lowered below the critical temperature of In (3.4 K) will there be nearly 100% Andreev reflection inside the In energy gap. Andreev reflection will still be imperfect in the energy range between the In and Nb gaps. We did not intentionally deposit In in the growth chamber, instead using the bonding wires to the sample to form that portion of the superconducting contact.

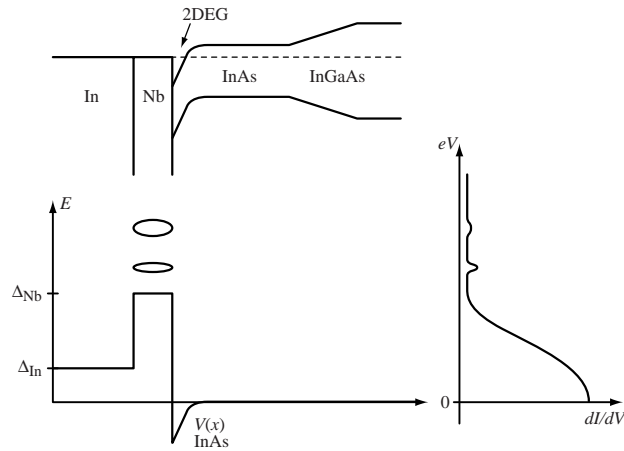


**Fig. 3.** Energy band diagram for a superconductor (In/Nb) to InAs contact. The negative Schottky barrier is shown as a triangular potential well near the surface. Expected differential conductance of the sample, including tunneling through the thin Nb and above barrier resonances, is shown on the right.

## 2.1. Superconductor to LTG-GaAs

The measured differential conductance from two different In/Nb–LTG-GaAs samples is shown in Figs 4–5. In both samples, we observe multiple subgap peaks corresponding to the McMillan–Rowell resonances. The subgap resonances are much clearer in Fig. 4, though they are also present in Fig. 5. One can even distinguish the two different energy gaps of In and Nb by the two different heights of the conductance resonances in Fig. 4. The larger peaks near zero bias correspond to the thick In layer, while the weaker peaks above the energy gap of In correspond to weaker Andreev reflection from the thin Nb superconductor (in addition to some Andreev reflection outside the In energy gap).

The McMillan–Rowell resonances in Fig. 5 are not as well developed as the ones in Fig. 4. ‘Sample 2’ may have an irregular contact geometry, with interface roughness broadening the Andreev resonances. ‘Sample 2’ may also consist of a series of more closely spaced conductance resonances which are not resolved at the base temperature of  $T = 1.6$  K. Both samples, we believe, are NINS junctions, with ‘Sample 2’ being a lower quality (broadened) version of ‘Sample 1’. Note that the Nb critical temperature is not 10 K in these samples, due to the compromises necessary to deposit Nb on the semiconductor structure.

Both LTG-GaAs samples were exposed to air prior to depositing Nb. To form ballistic Nb–LTG-GaAs interfaces, we relied on the well-known resistance of LTG-GaAs surfaces to oxidation. The appearance of Andreev resonances in both samples indicates a low degree of surface oxidation. It is remarkable that these samples show little indication of surface oxidation, even after exposure to air. The differences between these two nominally identical samples also shows the sensitivity of differential conductance spectroscopy using superconducting contacts. Several additional samples were measured, giving results similar to those shown in Figs 4–5.

## 2.2. Superconductor to InAs

Fig. 6 shows the differential conductance characteristics of two nominally identical In/Nb to InAs junctions. ‘Sample 3’ (top) shows an enhancement of conductance around zero voltage bias at the base temperature (1.6 K). In the BTK model [1], such an enhanced conductance near zero bias is associated with near ballistic transport of Cooper pairs through the normal-metal (InAs)/superconductor (Nb) interface. We

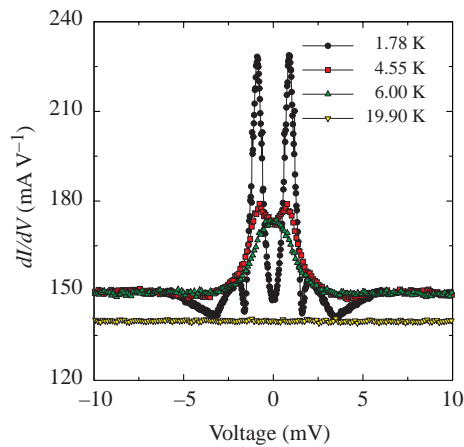


**Fig. 4.** Clear McMillan–Rowell subgap resonances in LTG-GaAs ‘Sample 1’ confirm the presence of an NINS junction. Therefore, only a small (or no) tunnel barrier is present at the superconductor/LTG-GaAs interface.

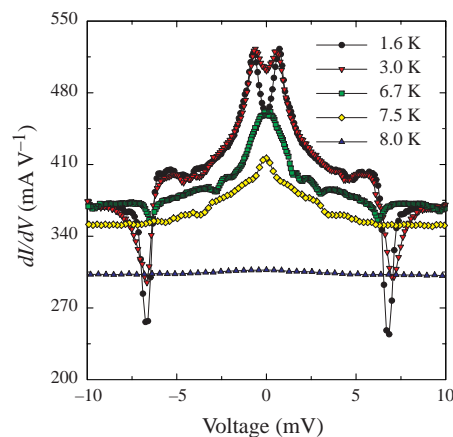


**Fig. 5.** ‘Sample 2’ is a superconductor/LTG-GaAs junction prepared identically to ‘Sample 1’. The subgap resonances are weaker and much broader, with an additional large drop in the differential conductance near 6.5 meV. Both features suggest an inhomogeneous contact geometry in this sample 2.

see the zero bias peak develop only as the In becomes superconducting, since the Nb layer is thin compared to the size of a Cooper pair. ‘Sample 4’ (bottom) displays Giaever tunneling. One can clearly see the In gap developing between 5.6 and 1.6 K in ‘Sample 4’. The Giaever tunneling peaks due to the Nb remain relatively unaffected as the temperature varies. The differential conductance of ‘Sample 4’ does not go to zero inside the gap, since the interface transmission of this tunnel barrier is of order  $T \simeq 0.1$ , as opposed to  $T = 10^{-6}$  in typical NIS tunnel junctions.

To avoid the formation of interface oxides before Nb deposition, we moved the wafer *in situ* (under high vacuum) after InAs growth to a Nb sputtering chamber. We did no additional surface cleaning, such as striking a plasma, prior to Nb deposition. The results in Fig. 6 indicate this procedure is only partially successful, since there is some variance in interface transmission from one sample to the next. We measured several additional samples, with differential conductance results similar to those in Fig. 6.

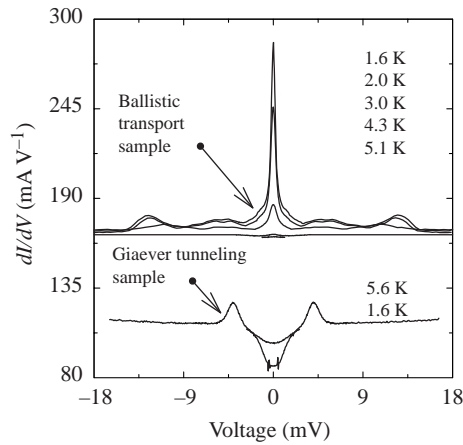


**Fig. 6.** Two identically prepared superconductor/InAs junctions. ‘Sample 3’ (top) exhibits ballistic transport of Cooper pairs across the interface to the semiconductor as the In becomes superconducting. ‘Sample 4’ (bottom) displays a modified Giaever tunneling in which one can also clearly see the development of the In gap.

### 2.3. Sample geometry and series resistance

A few caveats are necessary when attempting to extract detailed information about the energy gaps of the Nb and In from the measured data. The actual semiconductor samples are simply two metal Nb pads deposited on the semiconductor, together with their In bonding wires. Since the pad separation is  $10\ \mu\text{m}$ , the actual sample geometry is two large NS junctions in series (back-to-back). The energy gaps one infers from Figs 4–6 are larger than those of In and Nb due to the series resistance of the semiconductor connecting the two NS junctions. Series resistance is significant in Figs 4–6, since the NS junctions are low resistance, rather than high resistance (NIS) tunnel junctions. The actual sample geometry and sample preparation (growth) is described in detail elsewhere [35].

Series resistance stretches the voltage axis (makes the energy gaps and peak widths appear larger) and compresses the differential conductance (reduces relative heights of the peaks and valleys). Measurements of series resistance can be made using a transmission line structure, but we did not perform such measurements. We therefore cannot make quantitative comparisons of the data with a BTK-type conductance calculation. We can, however, make qualitative comparisons of theory and experiment as done in the next section.

## 3. Simulation

We simulate the differential conductance  $dI/dV$  at zero temperature using the BTK formula

$$\frac{dI}{dV} = \frac{2e}{h} [1 - R_e(E) + R_h(E)] dE. \quad (1)$$

Here  $R_e(E)$  is normal reflection probability and  $R_h(E)$  is the Andreev reflection probability. In this paper, we wish to model electron transport through the pairing potential

$$\Delta(x) = \begin{cases} 0 & x < 0, \\ \Delta_{\text{Nb}} & 0 < x < W, \\ \Delta_{\text{In}} & W < x. \end{cases} \quad (2)$$

The ordinary electrostatic potential we take as an impulse function located a distance  $L$  away from the Nb, namely

$$V(x) = V_0 \delta(x + L). \quad (3)$$

This combination of pairing and electrostatic potentials forms an of NINS junction. We can therefore use the reflection amplitudes  $r_e$  and  $r_h$  calculated in Ref. [2].

The only difference between the present calculation and that of Ref. [2] is the form of the pairing potential in the superconducting contact. We can modify calculation of Ref. [2] to account for the composite Nb/In contact by the following scheme: since the quantity  $(v_0/u_0) \exp(-i\phi)$  in eqns (A22)–(A26) of Ref. [2] corresponds to the Andreev reflection probability of an electron from the NS interface, we simply replace it by the Andreev reflection probability  $r_{a,e}$  from our new NS'S interface. The new reflection amplitudes are therefore

$$r_e = \frac{1}{d} \left( \frac{-iZ}{1+iZ} \right) [1 - (r_{a,e} r_{a,h}) e^{2i(k_+ - k_-)L}], \quad (4)$$

$$r_h = \frac{1}{d} (r_{a,e}) \left( \frac{1}{1+Z^2} \right) e^{i(k_+ - k_-)L}, \quad (5)$$

$$d = 1 - \left( \frac{Z^2}{1+Z^2} \right) (r_{a,e} r_{a,h}) e^{2i(k_+ - k_-)L}. \quad (6)$$

We then separately calculate the new Andreev reflection probability  $r_{a,e}$  from the composite Nb/In pairing potential step. The Andreev reflection amplitude of an electron from the pairing potential in eqn (2) we find to be

$$e^{i\phi} r_{a,e} = \frac{v_1}{u_1} + \left( 1 - \frac{v_1^2}{u_1^2} \right) r_{\text{step}} \left[ 1 + \left( \frac{v_1}{u_1} \right) r_{\text{step}} \right]^{-1}, \quad (7)$$

where

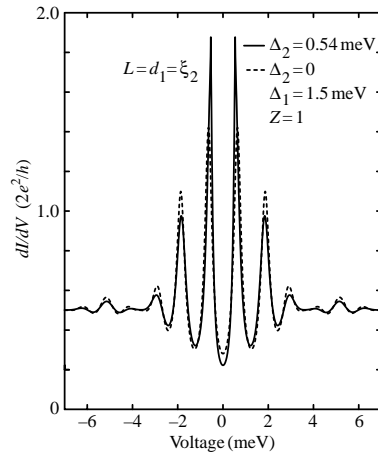
$$r_{\text{step}} = \left( \frac{v_2 u_1 - u_2 v_1}{u_2 u_1 - v_2 v_1} \right) \exp[i(k_{e1} - k_{h1})W]. \quad (8)$$

The Andreev reflection probability for holes we find as  $e^{i\phi} r_{a,e} = e^{-i\phi} r_{a,h}$ . The particle current reflection probabilities are then  $R_e(E) = |r_e|^2$  and  $R_h(E) = |r_h|^2$ .

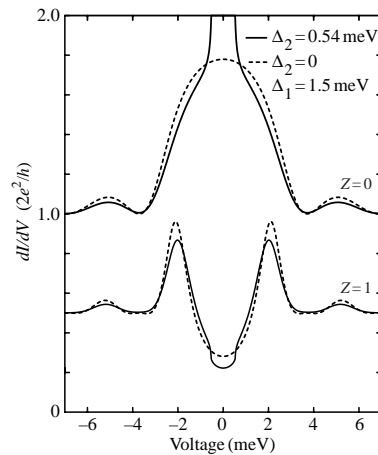
Plots of the differential conductance from eqn (1), using the Andreev reflection probabilities from eqns (4)–(8), are shown in Figs 7-8. Figure 7 models the LTG-GaAs junction, while Fig. 8 simulates the InAs junction. Solid lines give then conductance when the In is superconducting, while dashed lines simulate a normal In contact. We have not included thermal broadening in Figs 7–8.

Figure 7 reproduces most of the qualitative features of the differential conductance taken on the LTG-GaAs semiconductor. McMillan–Rowell type resonances occur inside the energy gap of both superconductors, but those inside the In gap become much stronger when the In goes superconducting. It is interesting that the height of some resonance peaks outside the In gap actually decrease (in this simulation) when the In becomes superconducting. We did not clearly observe this in the experiment. The calculation also shows weaker above barrier resonances not observed in experiment. (In Fig. 7 we have chosen the Nb layer thickness ( $W = d_1$ ) equal to the coherence length of the In ( $\xi_2$ ), even though the Nb is slightly thinner in the actual experiment. We have also arbitrarily set the spacing between the tunnel barrier to the Nb interface  $L = \xi_2$ .)

The simulation in Fig. 8 also confirms the qualitative features we observed in the differential conductance of the InAs semiconductor. The ballistic junction (top) corresponds to  $Z = 0$  in Fig. 8, while  $Z = 1$  corresponds to a tunnel junction (bottom) with barrier transmission 1/2. The transmission coefficient of the junction in its normal state is  $T = 1/(1 + Z^2)$ . A large peak in the differential conductance near zero bias appears in the ballistic junction when the In becomes superconducting. The ‘envelope’ of Andreev reflections also decreases somewhat outside the energy gap, which we did not observe in experiment, but is consistent with the simulation in Fig. 7. The two different energy gaps of In and Nb are also apparent in the tunnel junction in Fig. 8 (bottom).



**Fig. 7.** Numerical calculation of differential conductance corresponding to the In/Nb to LTG-GaAs junction. Strength of the McMillan–Rowell resonances inside the In gap increase as the In becomes superconducting. Solid lines give the differential conductance when the In becomes superconducting.



**Fig. 8.** Numerical calculation of differential conductance corresponding to the In/Nb to InAs junction. Effect of the In becoming superconducting can be seen both in the ballistic junction (top) and tunnel junction (bottom). Solid lines give the differential conductance when the In becomes superconducting.

#### 4. Conclusions

We have utilized differential conductance  $dI/dV$  versus voltage  $V$  in superconductor/semiconductor contacts as a very sensitive probe for the energy dependence of current carrying states in the junction. The superconducting contact is a composite of thin Nb with thick In, allowing us to probe with two different energy scales near the contact Fermi level. Since the Nb thickness is less than the Cooper pair size in Nb, the Nb forms only a partial Andreev mirror. Complete Andreev reflection occurs only from the thick In portion of the contact.

Junctions between In/Nb and InAs show ballistic transport at the NS interface, evidenced by the development of a large peak in the differential conductance near zero bias when the In becomes superconducting. Junctions between In/Nb and LTG-GaAs show McMillan–Rowell (NINS) type resonances. The resonances

become stronger inside the In energy gap when the In becomes superconducting, since the thick In now makes an effective Andreev mirror. Formation of such NINS resonances suggests a band of conducting states inside the energy gap of LTG-GaAs. Interface roughness, series resistance, and the actual three-dimensional contact geometry broaden and weaken features in the differential conductance, in comparison with an idealized one-dimensional scattering theory.

*Acknowledgements*—We wish to acknowledge the financial support from the David and Lucile Packard Foundation and from The MRSEC of the National Science Foundation under grant No. DMR-9400415. We thank Supriyo Datta, Michael McElfresh, and Richard Riedel for many useful discussions.

### References

- [1] G. E. Blonder, M. Tinkham, and T. M. Klapwijk, Transition from metallic to tunneling regimes in superconducting microconstrictions: excess current, charge imbalance, and supercurrent conversion, *Phys. Rev.* **B25**, 4515 (1982).
- [2] R. A. Riedel and P. F. Bagwell, Current–voltage relation of a normal metal–superconductor junction, *Phys. Rev.* **B48**, 15198 (1993).
- [3] S. Chaudhuri and P. F. Bagwell, Andreev resonances in the current–voltage characteristics of a normal metal–superconductor junction, *Phys. Rev.* **B51**, 16936 (1995).
- [4] A. M. Marsh, D. A. Williams, and H. Ahmed, Granular superconducting contacts to GaAs:AlGaAs semiconductor heterostructures, *Semicond. Sci. Technol.* **10**, 1694 (1995).
- [5] D. A. Williams, A. M. Marsh, and H. Ahmed, Transport through superconductor–semiconductor junctions in different scattering limits, *Surf. Sci.* **361/362**, 324 (1996).
- [6] J. R. Gao, J. P. Heida, B. J. van Wees, S. Bakker, T. M. Klapwijk, and B. W. Alphenaar, Low temperature current transport of Sn–GaAs contacts, *Appl. Phys. Lett.* **63**, 334 (1993).
- [7] A. M. Marsh, D. A. Williams, and H. Ahmed, Multiple Andreev reflection in buried heterostructure alloy superconductor devices, *Physica* **B203**, 307 (1994).
- [8] K. M. H. Lenssen, L. A. Westerling, C. J. P. M. Harmans, J. E. Mooij, M. R. Leys, W. vander Vleuten, and J. H. Wolter, Influence of gate voltage on the transport properties of superconducting/2DEG systems, *Surf. Sci.* **305**, 476 (1994).
- [9] J. R. Gao, J. J. B. Kerkhof, M. Verweft, P. Magnee, B. J. van Wees, T. M. Klapwijk, and J. Th. M. De Hosson, Analysis of superconducting Sn/Ti contacts to GaAs/AlGaAs heterostructures by electron focusing, *Semicond. Sci. Technol.* **11**, 621 (1996).
- [10] W. Poirier, D. Mailly, and M. Sanquer, Finite bias anomaly in the subgap conductance of superconductor–GaAs junctions, *Phys. Rev. Lett.* **79**, 2105 (1997).
- [11] J. Kutchinsky, R. Taboryski, T. Clausen, C. B. Sorensen, A. Kristensen, P. E. Lindelof, J. Bind-slev Hansen, C. Schelde Jacobsen, and J. L. Skov, Decay lengths for diffusive transport activated reflections in Al/n-GaAs/Al superconductor–semiconductor–superconductor contacts, *Phys. Rev. Lett.* **78**, 931 (1997).
- [12] V. I. Barrchukova, V. N. Gubankov, E. N. Enyushkina, S. A. Kovonyuk, I. L. Lapitskaya, M. P. Lisitskii, A. D. Maksimov, V. G. Mokerov, A. V. Nikiforov, and S. A. Shmelev, Preparation of  $n^{++}$  GaAs–Nb contacts and their electrophysical properties at low temperatures, *Tech. Phys. Lett.* **21**, 208 (1995).
- [13] A. M. Marsh, D. A. Williams, and H. Ahmed, Supercurrent transport through a high-mobility two-dimensional electron gas, *Phys. Rev.* **B50**, 8118 (1994).
- [14] A. J. Rimberg, T. R. Ho, C. Kurdak, and John Clarke, Dissipation-driven superconductor–insulator transition in two-dimensional Josephson junction array, *Phys. Rev. Lett.* **78**, 2632 (1997).
- [15] S. Chaudhuri, P. F. Bagwell, D. McInturff, J. C. P. Chang, S. Paak, M. R. Melloch, J. M. Woodall, T. M. Pekarek, and B. C. Crooker, Is the ‘finite bias anomaly’ in planar GaAs–superconductor junctions caused by point-contact-like structures, *Superlatt. Microstruct.* **25**, 745 (1999).

- [16] M. R. Melloch, J. M. Woodall, E. S. Harmon, N. Otsuka, F. H. Pollak, D. D. Nolte, R. M. Feenstra, and M. A. Lutz, Low-temperature grown III-V materials, *Ann. Rev. Mater. Sci.* **25**, 547 (1995).
- [17] R. M. Feenstra, J. M. Woodall, and G. D. Petit, Observation of bulk defects by scanning tunneling microscopy and spectroscopy: arsenic antisite defects in GaAs, *Phys. Rev. Lett.* **71**, 1176 (1993).
- [18] M. P. Patkar, T. P. Chen, J. M. Woodall, M. S. Lundstrom, and M. R. Melloch, Very low resistance nonalloyed ohmic contacts using low-temperature molecular beam epitaxy of GaAs, *Appl. Phys. Lett.* **66**, 1412 (1995).
- [19] H. Kroemer, C. Nguyen, and E. L. Hu, Ballistic electron transport and super conductivity in mesoscopic Nb–(InAs/AlSb) quantum well heterostructures, Paper presented at *Int. Symp. Compound Semiconductors, San Diego, 18–22 September 1994*.
- [20] B. J. van Wees, A. Dimoulas, J. P. Heida, T. M. Klapwijk, W. v.d. Graaf, and G. Borghs, Supercurrent transport and quasiparticle interference in mesoscopic two-dimensional electron gas coupled to superconductors, *Physica* **B203**, 285 (1994).
- [21] T. M. Klapwijk, Mesoscopic transport of InAs-based conductors with superconducting electrodes, *J. Low Temp. Phys.* **106**, 311 (1997).
- [22] S. G. den Hartog, C. M. A. Kapteyn, B. J. van Wees, T. M. Klapwijk, and G. Borghs, Transport in multi-terminal normal–superconductor devices: reciprocity relations, negative and nonlocal resistance, and reentrance of the proximity effect, *Phys. Rev. Lett.* **77**, 4954 (1996).
- [23] T. M. Klapwijk, Mesoscopic superconductor–semiconductor heterostructures, *Physica* **B197**, 481 (1994).
- [24] H. Takayanagi, T. Akazaki, J. Nitta, and T. Enoki, A Josephson field effect transistor using an InAs-inserted-channel  $\text{In}_{0.52}\text{Al}_{0.48}\text{As}/\text{In}_{0.53}\text{Ga}_{0.47}\text{As}$  inverted modulation-doped structure, *Appl. Phys. Lett.* **68**, 418 (1996).
- [25] H. Takayanagi, T. Akazaki, J. Nitta, and T. Enoki, Superconducting three-terminal devices using an InAs-based two-dimensional electron gas, *Jpn J. Phys.* **34**, 1391 (1995).
- [26] H. Takayanagi, T. Akazaki, J. Nitta, and T. Enoki, Submicron gate-fitted superconducting junction using a two-dimensional electron gas, *Jpn J. Appl. Phys.* **34**, 6977 (1995).
- [27] H. Kroemer and M. Thomas, Induced superconductivity in InAs quantum wells with superconductor–semiconductor contacts, *Superlatt. Microstruct.* **21**, 61 (1997).
- [28] M. Thomas, H. Blank, K. C. Wong, C. Nguyen, H. Kroemer, and E. L. Hu, Flux-periodic resistance oscillations in arrays of superconducting weak links based on InAs–AlSb quantum wells with Nb electrodes, *Phys. Rev.* **B54**, R2311 (1996).
- [29] A. Chrestin, T. Matsuyama, and U. Merkt, Evidence for a proximity-induced energy gap in N/InAs/Nb junctions, *Phys. Rev.* **B55**, 8457 (1997).
- [30] H. Drexler, J. G. E. Harris, E. L. Yuh, K. C. Wong, S. J. Allen, E. G. Gwinn, H. Kroemer, and E. L. Hu, Superconductivity and the Josephson effect in a periodic array of Nb–InAs–Nb junctions, *Surf. Sci.* **361/362**, 306 (1996).
- [31] S. G. Lachenmann, A. Kastalsky, I. Friedrich, A. Foster, and D. Uhlisch, Properties of Nb/InAs/Nb hybrid step junctions, *J. Low Temp. Phys.* **106**, 321 (1997).
- [32] M. Inoue, T. Sugihara, T. Maemoto, S. Sasa, H. Dobashi, and S. Izumiya, Low-dimensional electron transport properties in InAs/AlGaSb mesoscopic structures, *Superlatt. Microstruct.* **21**, 69 (1997).
- [33] L. C. Mur, C. J. P. M. Harmans, J. E. Mooij, J. F. Carli, A. Rudra, and M. Ilgems, Experimental indication of supercurrents carried by opened transport channels, *Phys. Rev.* **B54**, R2327 (1996).
- [34] P. Magnee, S. G. den Hartog, B. J. Van Wees, T. Klapwijk, W. v.d. Graaf, and G. Borghs, Experimental determination of the quasiparticle decay length  $\xi_{qp}$  in diffusive superconducting quantum well, *Phys. Rev.* **B52**, R11630 (1995).
- [35] T. Rizk, M.S.E.E. thesis, Purdue University, West Lafayette, IN 47907, U.S.A. (1998)..